$K^{\pi}=4^{-}$ isomers and their rotational bands in ^{168,170}Er

C. Y. Wu, D. Cline, M. W. Simon, and R. Teng
Nuclear Structure Research Laboratory, Department of Physics, University of Rochester, Rochester, New York 14627, USA

K. Vetter
Nuclear Science Division, Lawrence Berkeley National Laboratory, Berkeley, California 94720, USA

M. P. Carpenter, R. V. F. Janssens, and I. Wiedenhöver
Physics Division, Argonne National Laboratory, Argonne, Illinois 60439, USA
(Received 11 June 2003; published 10 October 2003)

The half-life of the known $I,K^{\pi}=4^{-},4^{-}$ state in ^{170}Er has been measured to be 42.8±1.7 ns. The rotational band built on this isomer was excited inelastically up to spin 18^{-} by a ^{238}U beam at E_{lab}=1358 MeV. A similar band in ^{168}Er was extended to spin 15^{-}. The wave function of the isomeric state in ^{170}Er has been determined from the measured $|g_K-g_R|$ values, which were deduced from the intensity ratios of the $\Delta I=1$ to $\Delta I=2$ transitions within the band. The dominant component consists of a two-quasiproton configuration involving the Nilsson orbits $7/2^{-}$[523] and $1/2^{+}$[411]. In contrast, the two-quasineutron configuration involving the $7/2^{+}$[633] and $1/2^{-}$[521] Nilsson orbits constitutes the major component for the wave function of the $K^{\pi}=4^{-}$ isomer in ^{168}Er.

DOI: 10.1103/PhysRevC.68.044305 PACS number(s): 21.10.Tg, 21.10.Ky, 21.10.Re, 27.70.+q

I. INTRODUCTION

The first excited band in ^{168}Er is the $K^{\pi}=2^{+}$, γ-vibrational band and the second one is the $K^{\pi}=4^{-}$ band with an excitation energy of 1094.0 keV [1]. The bandhead of the latter negative-parity band is an isomeric state with a half-life of 109 ns, which suggests that its wave function is dominated by the single-particle mode of motion rather than the collective modes. The wave function, measured by the (d,p) reaction [2], mainly consists of a two-quasineutron configuration involving the $7/2^{+}$[633] and $1/2^{-}$[521] Nilsson orbits. However, it was found later that a ≈30% admixture of the two-quasiproton configuration, involving the $7/2^{-}$[523] and $1/2^{+}$[411] Nilsson orbits, is required for the wave function to account for the measured g factor [3]. Therefore, both the neutron and proton configurations contribute to the underlying single-particle structure of the $I,K^{\pi}=4^{-},4^{-}$ state in ^{168}Er.

For ^{170}Er, a similar $K^{\pi}=4^{-}$ band has been tentatively identified with an excitation energy of 1268.6 keV [4]. It has been suggested [5] that the bandhead of this rotational band has a single-particle configuration similar to that of ^{168}Er; that is, the wave function mainly consists of the same two-quasineutron configuration involving the $7/2^{+}$[633] and $1/2^{-}$[521] orbitals with a possible smaller contribution from the two-quasiproton configuration involving the $7/2^{-}$[523] and $1/2^{+}$[411] orbitals. In this paper, we present new spectroscopic data for this $K^{\pi}=4^{-}$ band resulting from the study of inelastic excitation of ^{170}Er. The single-particle structure and the decay properties of the bandhead will be discussed by using the measured lifetime and g factor.

II. EXPERIMENT

The experiment was performed by bombarding ^{170}Er targets with a ^{238}U beam at E_{lab}=1358 MeV, provided by the ATLAS facility at the Argonne National Laboratory. The targets had a thickness between 320 and 540 μg/cm^2 and an ^{170}Er enrichment of ≈97%. The deexcitation γ rays were detected by Gammasphere [6], an array of 100 Compton-suppressed Ge detectors, in coincidence with both outgoing particles detected by the highly segmented parallel-plate avalanche detector array, CHICO [7]. Note that there were no heavymet shields mounted on the BGO Compton-suppression shields for this experimental setup. Details of the experiment and of the analysis have been described in an earlier publication [8], which addresses the issue of the complex band interactions in ^{170}Er. The present paper introduces a unique aspect of this setup for the study of isomers.

The reconstructed two-body kinematics, from the measured scattering angles for both recoiling nuclei and their time-of-flight difference, allows the determination of the masses of the reaction products, their velocity vectors, and the reaction Q value. From the deduced masses and velocity vectors, the appropriate Doppler-shift correction can be applied to the prompt γ rays and the distinction between γ rays originating from either reaction product can be made in a straightforward manner. The resulting γ rays have an energy resolution of ≈1.1%, which is limited mainly by the finite size of Ge detectors. Since both outgoing particles were stopped in the cathode boards of CHICO, the γ rays emitted by isomers with lifetimes longer than the target-cathode flight time, typically ≈10–15 ns, experience no Doppler shift. This feature can be used to distinguish delayed γ rays from prompt ones. An example is shown in Fig. 1, where the sharp peaks were recognized as delayed transitions in the raw spectrum obtained by requiring the arrival time of the γ rays to be at least 40 ns past the prompt coincident time. The efficiency to detect the delayed γ rays at the off-target position, calculated using the Monte Carlo code GEANT [9], changed at most by 10% relative to that for γ rays emitted at

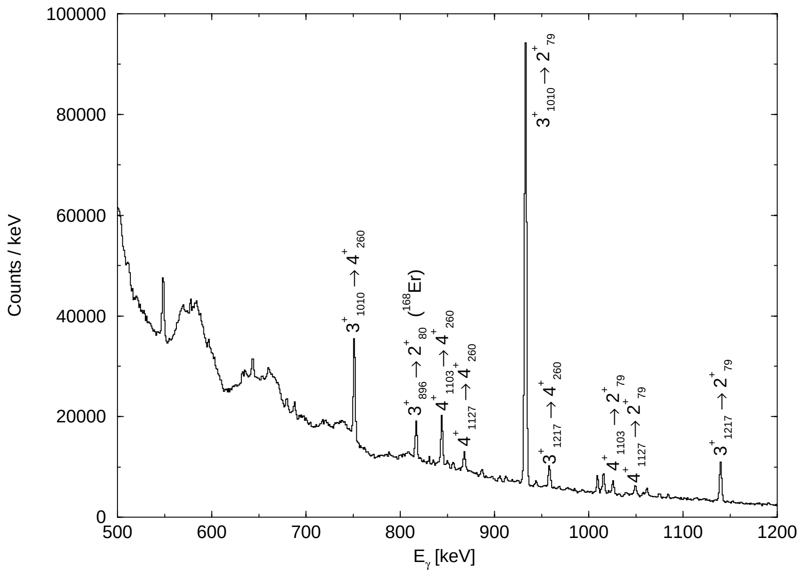

FIG. 1. The delayed γ-ray spectrum for the reaction between ^{170}Er and ^{238}U at $E_{\mathrm{c.m.}}$ =566 MeV, where c.m. stands for center of mass. The labeled peaks correspond to transitions following the isomeric decay of the K^{π}=4$^-$ state in ^{170}Er. The γ-ray transitions, following the isomeric decay of K^{π}=4$^-$ state in ^{168}Er, also were observed because of a $\approx$2% ^{168}Er contamination in the Er target.

the target position [10]. The assignment of the isomer to a particular reaction product is made by the cross correlations between the prompt and delayed γ rays, as illustrated in Fig. 2, where the pattern of the prompt γ rays, obtained by gating on the delayed γ rays, is presented.

III. RESULTS AND DISCUSSION

The I,K^{π}=4$^-$,4$^-$ state at 1268.6 keV in ^{170}Er was identified to be an isomer by the correlations between the known prompt γ rays from decays of the rotational band members, 5$^-$ and 6$^-$, and the delayed γ rays following the isomer decay, shown in Fig. 2. Its half-life was measured to be 42.8±1.7 ns from the spectrum measuring the time difference between γ rays and particles. Together with the known decay branching ratios [4], the E1 strengths to states of various K values were derived; these are listed in Table I.

As can be seen in Table I, the retarded transition rate for the allowed E1 transition to the I,K^{π}=3$^+$,3$^+$ state in ^{170}Er is of the order of 10^{-6} W.u. For the K forbidden E1 transitions, the systematics of the retardation of the transition rate is generally consistent with the degree of K-forbiddenness. This also is the case for transitions in ^{168}Er. There is one marked exception, namely, the transition to the I,K^{π}=4$^+$,0_2^+ state in ^{170}Er, where the transition rate is less retarded than that of the transition to the I,K^{π}=4$^+$,0_1^+ state by roughly four orders of magnitude and is comparable to the values measured for transitions leading to the K^{π}=2$^+$ states. As discussed in an earlier publication on ^{170}Er [8], a strong mixing, due to an accidental degeneracy, occurs between the two 4$^+$ states with K^{π}=0_2^+ and 2$^+$. This strong mixing leads to a reduction in the degree of K forbiddenness and a less retarded transition rate for the E1 transition between I,K^{π}=4$^-$,4$^-$ and I,K^{π}=4$^+$,0_2^+ states. Conversely, this less retarded transition rate supports the scenario of a strong mixing between the two 4$^+$ states.

The rotational band built on the K^{π}=4$^-$ isomer in ^{170}Er was identified and fully characterized from the prompt γ rays

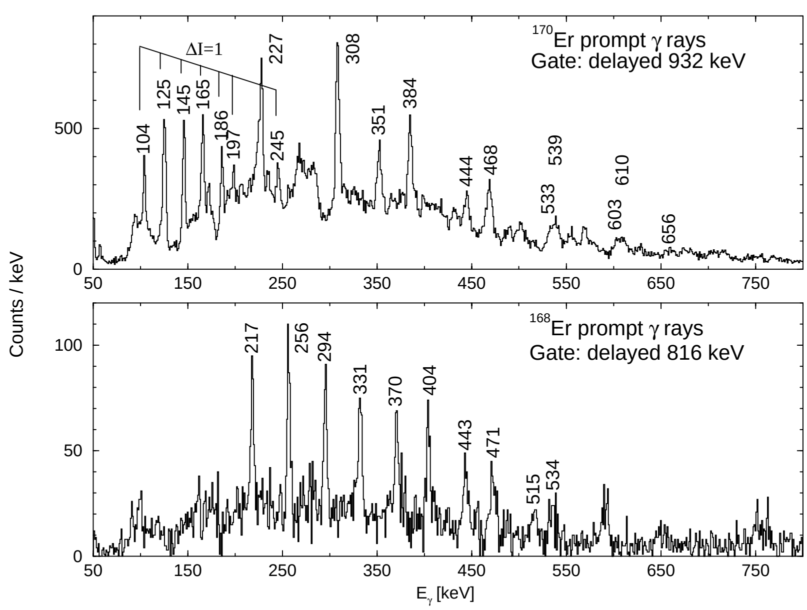

FIG. 2. Prompt coincidence spectra gated by the delayed γ-ray transitions following the isomeric decay of K^{π}=4$^-$ states of both ^{168}Er (lower) and ^{170}Er (upper). The ΔI=1 transitions are absent in ^{168}Er. The labeled transition energies are in keV. The coincidence gate for both isotopes is the delayed transition from the 3$^+$ state of the γ band to the 2$^+$ state of the ground-state band.

TABLE I. $E1$ strengths for the decay of $K^{\pi}=4^{-}$ states in ^{168,170}Er.

I_f,K_f	E_x (keV)		$B(E1)$ (W.u.)	
	^{168}Er	^{170}Er	^{168}Er[a]	^{170}Er
$4^+,0_1^+$	264.1	260.2	3.60×10^{-10}	1.37×10^{-11}
$4^+,0_2^+$		1103.4		1.25×10^{-7}
$3^+,2^+$	895.8	1010.6	2.07×10^{-7}	3.18×10^{-7}
$4^+,2^+$	994.8	1127.2	1.28×10^{-7}	0.88×10^{-7}
$3^+,3^+$		1217.4		2.82×10^{-6}

[a]From Ref. [1].

correlated with the delayed transitions following the isomer decay, and from the events where a minimum of three γ rays were detected in prompt coincidence. This band, together with that for ^{168}Er, is shown in Fig. 3. The transition energies for the intraband transitions are listed in Tables II and III, respectively, for ^{168}Er and ^{170}Er. The data on ^{168}Er resulting from the present work were derived from the inelastic excitation of a $\approx$2% contamination of ^{168}Er in the enriched ^{170}Er target. This accomplishment can be attributed to the high sensitivity achieved (which is of the order of 10^{-7} in the population probability) with the experimental setup, which had essentially 4π coverage for the detection of both γ rays and particles. The known level scheme of the $K^{\pi}=4^{-}$ isomeric band has been substantially extended for both isotopes; from spin 8^- at 1605.9 keV to 15^- at 3190.4 keV for ^{168}Er and from spin 7^- at 1640.5 keV to 18^- at 4446.8 keV for ^{170}Er.

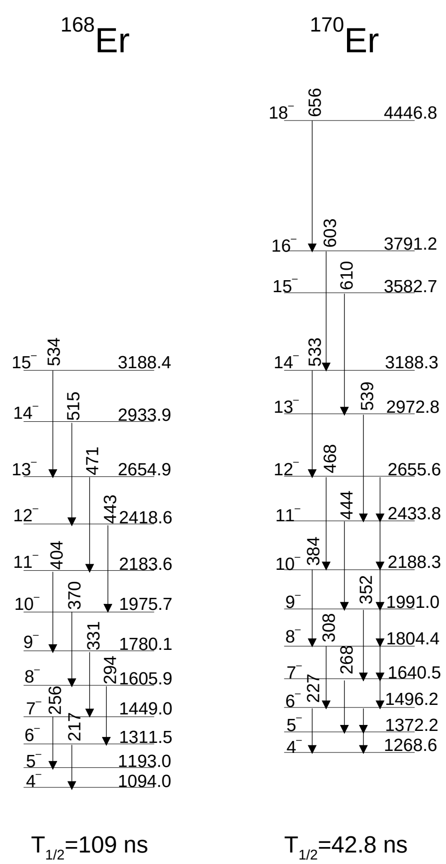

FIG. 3. Level schemes for the $K^{\pi}=4^{-}$ bands for both ^{168}Er and ^{170}Er. The energies are labeled in keV.

The characteristics of the $K^{\pi}=4^{-}$ rotational band for ^{170}Er are markedly different from those of its counterpart in ^{168}Er. For example, the energy staggering is more pronounced in ^{170}Er than in ^{168}Er, as shown in Fig. 4 where the moments of inertia versus the rotational frequency are plotted. This staggering also has the opposite even-odd spin dependence for the two isotopes. The most striking distinction between the two cases is the decay pattern of the intraband transitions, where the strength of the $\Delta I=1$ transitions is comparable to that of the $\Delta I=2$ transitions in ^{170}Er, while the $\Delta I=1$ transitions are weak in ^{168}Er, as shown in Fig. 2. The intensities for those weak $\Delta I=1$ transitions in ^{168}Er cannot be determined with any statistical significance in this work. This observation can be viewed as a strong indication of a marked difference in the intrinsic structure of the two bands.

The weak $\Delta I=1$ transitions in ^{168}Er can be attributed to the negligible $|g_K-g_R|$ value, where g_K and g_R are the g factors for the single-particle and rotational modes of motion, respectively. The g_K value for the $K^{\pi}=4^{-}$ state in ^{168}Er was measured to be 0.24±0.01 [3] and g_R can be taken approximately to be equal to the g factor of the first 2^+ state, which was measured to be 0.31±0.03 [3].

TABLE II. Transition energies and relative γ-ray intensities for the intraband transitions of the $K^{\pi}=4^{-}$ band in ^{168}Er. Uncertainty for the transition energy is $\approx$1 keV.

Transition	E_γ (keV)	Relative intensity	
		This work	Reference [1]
$6^-\to5^-$	118.5		0.24(3)
$6^-\to4^-$	217.2		1.00
$7^-\to6^-$	137.5		0.116(14)
$7^-\to5^-$	255.7		1.00
$8^-\to7^-$	156.9		0.049(10)
$8^-\to6^-$	294.4		1.00
$9^-\to7^-$	331.1		
$10^-\to8^-$	369.8		
$11^-\to9^-$	403.5		
$12^-\to10^-$	442.9		
$13^-\to11^-$	471.3		
$14^-\to12^-$	515.3		
$15^-\to13^-$	533.5		

TABLE III. Transition energies and relative γ-ray intensities for the intraband transitions of the $K^{\pi}=4^{-}$ band in ^{170}Er. Uncertainty for the transition energy is ≈ 1 keV.

Transition	E_{γ} (keV)	Relative intensity This work	Relative intensity Reference [4]
$6^{-}\rightarrow 5^{-}$	124.5	1.63(33)	1.00(23)
$6^{-}\rightarrow 4^{-}$	226.6	1.00	1.00
$7^{-}\rightarrow 6^{-}$	144.5		
$7^{-}\rightarrow 5^{-}$	268.0		
$8^{-}\rightarrow 7^{-}$	164.5	0.425(85)	
$8^{-}\rightarrow 6^{-}$	307.5	1.00	
$9^{-}\rightarrow 8^{-}$	185.5	0.50(12)	
$9^{-}\rightarrow 7^{-}$	351.5	1.00	
$10^{-}\rightarrow 9^{-}$	197.1	0.233(56)	
$10^{-}\rightarrow 8^{-}$	384.1	1.00	
$11^{-}\rightarrow 10^{-}$	244.6	0.57(15)	
$11^{-}\rightarrow 9^{-}$	443.6	1.00	
$12^{-}\rightarrow 11^{-}$	221.5	0.34(8)	
$12^{-}\rightarrow 10^{-}$	467.6	1.00	
$13^{-}\rightarrow 11^{-}$	539.0		
$14^{-}\rightarrow 12^{-}$	532.7		
$15^{-}\rightarrow 13^{-}$	609.9		
$16^{-}\rightarrow 14^{-}$	602.9		
$18^{-}\rightarrow 16^{-}$	655.6		

Under the assumption of a rotor model, the values of $|(g_K-g_R)/Q_0|$, where Q_0 is the intrinsic $E2$ moment, can be derived for the members of a rotational band directly from the measured intensity ratios between the ΔI=1 and Δ=2 transitions. The $|g_K-g_R|$ values deduced from these ratios for the transitions of $K^{\pi}=4^{-}$ band in ^{170}Er, which are listed in Table III, are given as a function of spin in Fig. 5 under the assumption that Q_0 is equal to that of the ground-state band, 7.64 b [4]. Note that the intensity ratio of the ΔI=1 to ΔI =2 transitions from the current measurement for the 6^{-} state

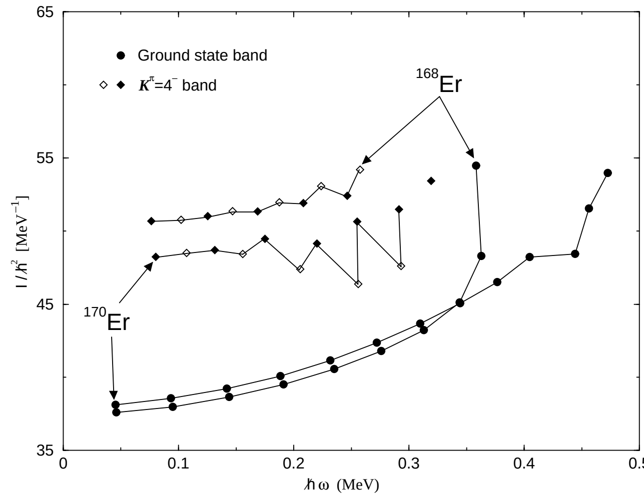

FIG. 4. The kinematic moments of inertia as a function of rotational frequency for the ground-state and $K^{\pi}=4^{-}$ bands of both ^{168}Er and ^{170}Er. The 724.8 and 716 keV γ rays were assigned, for the first time, to the $18^{+}\rightarrow 16^{+}$ and $20^{+}\rightarrow 18^{+}$ transitions in ^{168}Er.

is 1.63±0.33 compared to the published value of 1.00±0.23 [4]. The lack of data for the 7^{-} state is because of the difficulty in determining accurately the intensity of the 268 -keV transition (see Fig. 2). As can be seen in Fig. 5, the $|g_K-g_R|$ values remain nearly constant up to the 10^{-} state and then rise suddenly for the 11^{-} state and above. This change at the 11^{-} state coincides with the change in the pattern observed also in the moment of inertia plot of Fig. 4. This phenomenon is presumably related to a mixing of the underlying single-particle structure for band members with spin 11^{-} and above.

For a state with a given two-quasiparticle configuration, the g_K can be calculated according to the additive theory given by the equation [11–13]

$$g_K = 1/2(g_1+g_2) + \{[j_1(j_1+1) - j_2(j_2+1)]/[2I(I+1)]\}(g_1-g_2), \quad (1)$$

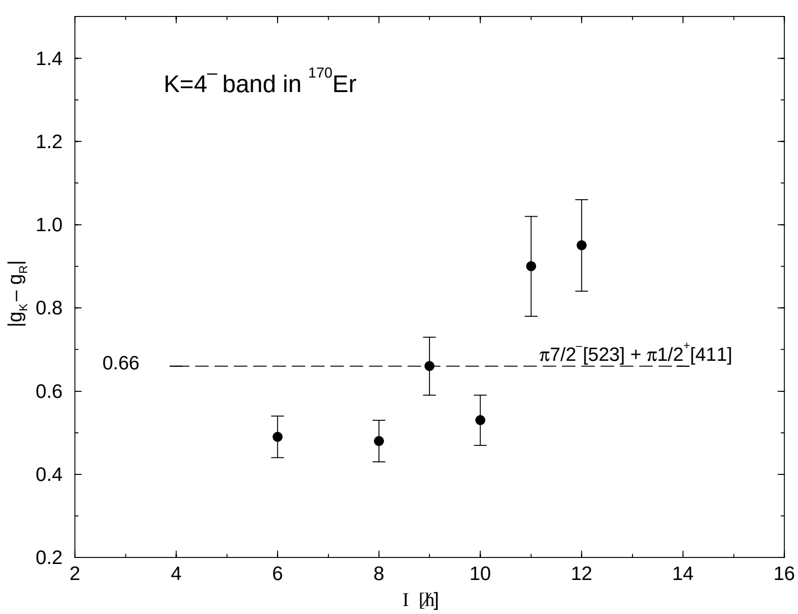

FIG. 5. The measured $|g_K-g_R|$ values plotted as a function of spin for the $K^{\pi}=4^{-}$ band in ^{170}Er assuming a pure K configuration. The values of 0.66, represented by the dashed lines, is the calculated $|g_K-g_R|$ value corresponding to the two-quasiproton configuration labeled.

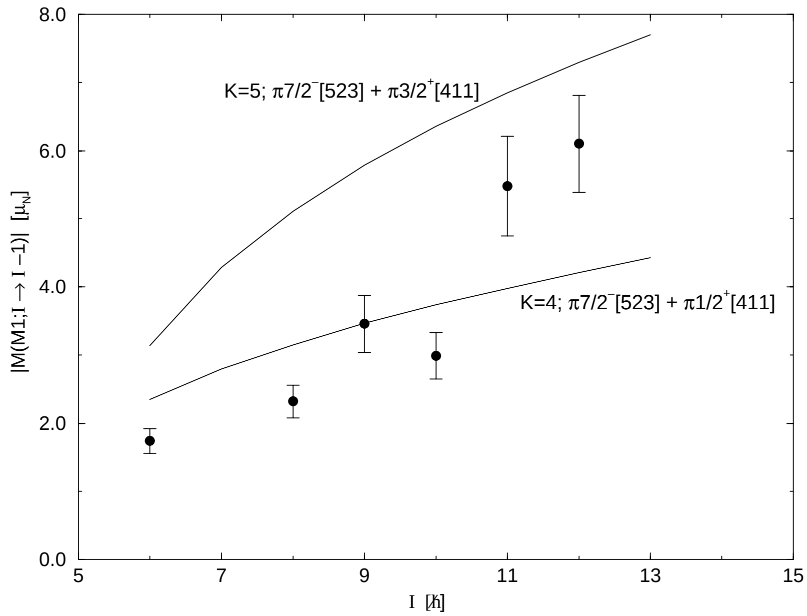

FIG. 6. The measured $|M(M1)|$ values plotted as a function of spin for the band built on the $K^{\pi}=4^{-}$ state in ^{170}Er. The solid lines are the calculated $|M(M1)|$ values corresponding to the two-quasiproton configurations labeled.

where g_K is the g factor for a state with spin I built from a two-quasiparticle configuration with spins j_1 and j_2 and g factors g_1 and g_2, respectively. The calculated g_K is -0.013 [3] for $K^{\pi}=4^{-}$ assuming that its two-quasiparticle configuration comprises the $7/2^{+}[633]$ and $1/2^{-}[521]$ neutron orbits. With a g_R value taken to be equal to the g factor of the first 2^{+} state (0.32) [14], this negligible g_K value leads to a upper bound, ≈ 0.32, for the value of $|g_K-g_R|$, which cannot account for the measured values. Thus, the underlying single-particle structure for the $K^{\pi}=4^{-}$ state in ^{170}Er cannot be dominated by these neutron states as suggested in Ref. [5]. The agreement between the measured $|g_K-g_R|$ values and the calculated ones is much improved if a two-quasiproton configuration involving $7/2^{-}[523]$ and $1/2^{+}[411]$ orbitals is assumed for the underlying single-particle structure. The calculated g_K value is 0.98 with $g(7/2^{-}[523],{}^{165}\mathrm{Ho})=1.18$ and $g(1/2^{+}[411],{}^{169}\mathrm{Tm})=-0.46$ adopted from Ref. [14] and leads to $|g_K-g_R|=0.66$. By comparing the measured $|g_K-g_R|$ to the calculated value, one can conclude that this two-quasiproton configuration constitutes nearly 90% of the wave function for the $K^{\pi}=4^{-}$ state in ^{170}Er.

The sudden rise in $|g_K-g_R|$ values for states with spin 11^{-} and above suggests a mixing of additional two-quasiparticle configurations. Three close-lying single-proton configurations, which could be the candidates in forming such two-quasiparticle configurations, are identified after examining the level schemes of ^{169}Ho and ^{171}Tm, the isotones of ^{170}Er. They are the $1/2^{+}[411]$, $3/2^{+}[411]$, and $7/2^{-}[523]$ proton orbitals. The coupling between the $1/2^{+}[411]$ and $7/2^{-}[523]$ orbitals constitutes the main component of the underlying single-particle structure for the low-spin states of $K^{\pi}=4^{-}$ band as discussed earlier. The perturbation to the higher-spin states could be due to mixing with the band members built on the $K^{\pi}=5^{-}$ state with the configuration involving the $3/2^{+}[411]$ and $7/2^{-}[523]$ orbitals. This configuration gives $g_K=1.27$ with $g(3/2^{+}[411],{}^{161}\mathrm{Tb})=1.47$ [14], which leads to $|g_K-g_R|=0.95$. Since K is no longer a good quantum number, the $M1$ matrix element, instead of the $|g_K-g_R|$ value, is the appropriate quantity for comparison between the experimental values and the theoretical prediction. The experimental $M1$ matrix elements together with the calculated ones from these two configurations are shown in Fig. 6. $A\approx 50-50$ mixing can account for the sudden rise of the measured $M1$ matrix elements and $|g_K-g_R|$ values.

In summary, the $K^{\pi}=4^{-}$ isomer in ^{170}Er has been populated by the inelastic scattering of ^{170}Er by a ^{238}U beam at near barrier energy. The isomer identity was established by the correlations between the prompt and delayed γ rays. With the prompt-delayed correlations and the events with at least three prompt γ rays, the rotational band built on the $K^{\pi}=4^{-}$ isomer has been extended substantially for ^{170}Er as well as for ^{168}Er. From the measured lifetime and the g factors, the decay properties and the underlying single-particle structure of the isomeric state have been discussed quantitatively. We conclude that the two-quasiproton configuration involving the $7/2^{-}[523]$ and $1/2^{+}[411]$ orbitals is the dominant component for the underlying structure in ^{170}Er. This contradicts the conclusion of Ref. [5], which associates the isomer with the two-quasineutron configuration involving the $7/2^{+}[633]$ and $1/2^{-}[521]$ orbits. Significant mixing of an additional two-quasiproton configuration involving the $3/2^{+}[411]$ and $7/2^{-}[523]$ orbitals for states with the rotational frequency above ≈ 200 keV may be responsible for the rise in the measured g factors.

ACKNOWLEDGMENTS

We thank Dr. I. Ahmad and Dr. J. P. Greene for making and handling the ^{252}Cf source for the CHICO calibration. The work by the Rochester group was funded by the National Science Foundation. The work at LBNL and ANL was performed under the auspices of the U.S. Department of Energy under Contract Nos. DE-AC03-76SF00093 (LBNL) and W-31-109-ENG-38 (ANL).

[1] V. S. Shirley, Nucl. Data Sheets **71**, 261 (1994), and references therein.

[2] R. A. Harlan and R. K. Sheline, Phys. Rev. **160**, 1005 (1967).

[3] A. Furusawa, M. Kanazawa, and S. Hayashibe, Phys. Rev. C **21**, 2575 (1980).

[4] C. M. Baglin, Nucl. Data Sheets **96**, 611 (2002), and references therein.

[5] E. P. Grigoriev and I. A. Gladkova, Yad. Fiz. **63**, 733 (2000) [Phys. At. Nucl. **63**, 705 (2000)].

[6] I. Y. Lee, in *Proceedings of the Workshop on Gammasphere Physics, Berkeley, CA*, edited by M. A. Deleplanque, I. Y. Lee, and A. O. Macchiavelli (World Scientific, Singapore, 1996), p. 50.

[7] M. W. Simon, D. Cline, C. Y. Wu, R. W. Gray, R. Teng, and C. Long, Nucl. Instrum. Methods Phys. Res. A **452**, 205 (2000).

[8] C. Y. Wu, D. Cline, M. W. Simon, R. Teng, K. Vetter, M. P. Carpenter, R. V.F. Janssens, and I. Wiedenhöver, Phys. Rev. C **61**, 021305(R) (2000).

[9] R. Brun, F. Bruyant, M. Maire, A. C. McPherson, and P. Zanarini, GEANT, version 3.159, GEANT3 User's Guide, DD/EE/84-1, CERN, 1987.

[10] M. W. Simon, Ph.D. thesis, University of Rochester, 1999.

[11] E. Ejiri, G. B. Hagemann, and T. Hammer, in *Proceedings of the International Conference on Nuclear Moment and Nuclear Structure*, edited by H. Horie and K. Sugimoto (Physical Society of Japan, Tokyo, 1972), p. 428.

[12] E. Bodenstedt, Hyperfine Interact. **2**, 1 (1976).

[13] P. J. Brussaard and P. W.M. Glaudemans, *Shell Model Applications in Nuclear Spectroscopy* (North-Holland, Amsterdam, 1977), p. 256.

[14] R. B. Firestone, V. S. Shirley, C. M. Baglin, S. Y. F. Chu, and J. Zipkin, *Table of Isotopes*, 8th ed. (John Wiley & Sons, New York, 1996), Vol. II.